

Charge transfer and oxygen ordering in $\text{YBa}_2\text{Cu}_3\text{O}_{6+x}$

A. A. Aligia and J. Garcés

Comisión Nacional de Energía Atómica, Centro Atómico Bariloche, 8400 S.C. de Bariloche, Río Negro, Argentina

(Received 5 April 1993)

The electronic structure of the CuO_x planes is studied using a generalized Hubbard model including Cu-O repulsion U_{pd} , for each value of x and two different assumptions on the oxygen (O) ordering. The result explains qualitatively the experimentally observed hole count in the CuO_2 planes, the amount of Cu^+ and the metal-insulator transition near $x=0.5$. For large enough U_{pd} , the energy ΔE favoring ordering in chains is positive. A simple explanation of this and the relation between charge transfer and O ordering is given. The screening length λ is calculated using Thomas-Fermi theory, an effective one-band model for the CuO_2 planes and experimental data. This information is used to construct an effective lattice-gas model for the O ordering, based on O-O screened repulsions in which ΔE is the only parameter. The superstructures predicted by this model provide an explanation of almost all observed diffraction patterns and of recently observed photoinduced changes in the transport properties. The electronic and structural results are consistent with the observed dependence of the superconducting T_c vs x .

I. INTRODUCTION

In spite of recent experimental and theoretical progress, the electronic structure of high- T_c systems is not completely understood yet. This is mainly due to the large magnitude of the correlations in the problem, and the present shortcomings of theoretical methods used to handle strongly correlated systems. Since the O ordering is ultimately determined by the electronic structure of the system, one cannot expect a complete understanding of the former either. However, theoretical studies of the relation between the electronic and the atomic structure of $\text{YBa}_2\text{Cu}_3\text{O}_{6+x}$ (Refs. 1–7) were successful in clarifying some of the most important aspects. Experimentally, it is clear that when quenched samples of $\text{YBa}_2\text{Cu}_3\text{O}_{6+x}$ with oxygen content $x \sim 0.5$ are annealed at room temperature, the superconducting T_c increases.^{8–10} This effect was interpreted as due to a reordering of the O atoms of the CuO_x planes in such a way that two threefold coordinated Cu ions of these planes are transformed into one fourfold and one twofold coordinated Cu ion. This picture has been confirmed by optical measurements.¹¹ A simple argument, valid in the extremely strong-coupling limit, which explains why this reordering dopes the CuO_2 planes and at the same time why this charge transfer favors energetically the ordering in chains, is given at the beginning of Sec. II.

Among the electronic properties which are characteristic of $\text{YBa}_2\text{Cu}_3\text{O}_{6+x}$, the most salient are the plateaus in the x dependence of T_c (Refs. 12–15) and number of carriers n_H deduced from Hall measurements,^{14–16} and the metal-insulator transition near $x \sim 0.5$.^{14,15,17,18} The magnetic properties¹⁸ and low-temperature transformations possibly related with the formation of ferroelectric and antiferroelectric domains¹⁹ also distinguish this system from the other high- T_c ones. An important clue in the understanding of the electronic structure is provided

by optical experiments which determine the amount of Cu^+ .^{20,21} It behaves like $1-2x$ for $x \leq 0.2$ and like $1-x$ for $x \geq 0.4$. This result agrees with ^{63}Cu nuclear quadrupole resonance (NQR) experiments for $x \cong 2/3$.²² The first plateau in T_c vs x , for $0.6 < x \lesssim 0.75$ with $T_c \sim 60$ K is related to the corresponding plateau in n_H vs x , while the second plateau in T_c , for $0.8 < x < 1$ with $T_c \sim 90$ K is due to the fact that, although n_H still increases with x , T_c vs n_H passes through its maximum value.^{23–27}

The first explanation of the plateau in n_H vs x was a “weak-coupling” one.²⁸ It was assumed that O vacancies enter in full CuO chains in a regularly spaced form. However, the energy calculated with the same model they propose, and experimental evidence in the region of the plateau,^{22,29–32} suggest that the CuO chains are intact. Diffraction patterns originated from regularly spaced vacancies were observed only for $x \geq 3/4$.^{13,33} In addition, due to the neglect of correlations, the model cannot explain the x dependence of the amount of Cu^+ and the semiconducting behavior for $x < 1/2$. Instead, a semi-quantitative agreement with the observed x dependence of both n_H and the amount of Cu^+ was obtained using strong-coupling approaches to the electronic structure of the CuO_x planes.^{1,34,35,6,36} The first approach included the apex O ions [O(1) in the notation of Ref. 37] and also obtained a metal-insulator transition at $x=0.5$ and the energy ΔE which favors ordering in CuO chains. The model is described in Sec. II and briefly in Refs. 1 and 34. The basic assumptions are the following: (1) The system composed of the CuO_x planes and the apex O atoms is “disconnected” from the superconducting planes. This is supported by band-structure calculations.^{38–40} (2) Intra-atomic correlations are so strong that Cu^{+3} and neutral O^0 are absent. (3) The system can be described by an extended Hubbard model and doped infinite chains are described by an effective Hamiltonian with all Cu ions as Cu^{+2} . The approach of Uimin *et al.*^{6,36} is similar.

However these authors neglected the apex O(1) atoms, and different properties are explained in terms of a large statistical amount of short CuO chains. We believe that unless long-range O-O repulsions are included^{1,41,42} infinite CuO chains will always be stable below room temperature.

At temperatures above room temperature, the O ordering in the CuO_x planes is characterized by three phases: tetragonal (TG), orthorhombic (OI), and double-cell orthorhombic (OII).⁴³⁻⁴⁵ At lower temperatures not only these phases, but several other superstructures (SS) have been observed by electron diffraction. For ideal compositions in the range $1/2 \leq x \leq 3/4$, they correspond to arrangements of full and empty CuO chains, with unit cell $1 \times n$ with $n \leq 8$ ²⁹⁻³³ We call them "chain structures" (CS). For ideal compositions $x \leq 3/8$ (Refs. 33 and 29) [$x \geq 3/4$ (Refs. 13 and 33)], SS have been reported in which the O atoms (vacancies) tend to be as far apart as possible. These diffraction patterns are compatible with the SS which minimize the interatomic O-O repulsion.^{1,41,42,46} We call them HS because they often resemble a deformed hexagonal lattice. The general aspect of the SS with ideal compositions $x=1/2$ and $x=3/8$ has been confirmed by neutron⁴⁷⁻⁴⁹ and x-ray^{50,51,49,52} experiments. The structure of unit cell 1×3 with ideal composition $x = 2/3$ has also been confirmed by x-ray diffraction.⁵² There is a controversy about the other SS which will be addressed in Sec. IV.

A method which has been successful in the theoretical description of phase diagrams of binary transition-metal alloys is to use an effective lattice-gas (or Ising) model with parameters determined by fitting the energy of several structures (some of them hypothetical) to *ab initio* calculations.⁵³ In carbides and nitrides of transition metals a systematic error in the theoretical cohesive energy has been found.⁵⁴ This method is not expected to work in highly correlated systems. In particular, for insulating perovskites related to a high- T_c system, the *ab initio* calculations predict a metallic phase, unless the total-energy functional is modified.⁵⁵ The phase diagram for O ordering in $\text{YBa}_2\text{Cu}_3\text{O}_{6+x}$ above room temperature has been explained restricting the maximum interaction range *a priori* to one lattice parameter of the CuO_x planes.⁴⁵ The interactions which best fit the phase diagram are near to those obtained using a linear muffin-tin orbital (LMTO) calculation.⁵⁶ However, with these parameters, there are serious disagreements for chemical potential and molar enthalpy and entropy in $\text{ErBa}_2\text{Cu}_3\text{O}_{6+x}$.⁵⁷ The agreement on the phase diagram is probably fortuitous: on the one hand, the reduction of the energy when correlations are included using the Gutzwiller approximation [Eq. (14)], is of the order of 0.6 eV per unit cell, much larger than the calculated interactions and depends on the O ordering. On the other hand, the range of the interactions is at least two times the lattice parameter a . Repulsions at this distance are necessary⁵⁸ in the explanation of Khachatryan and Morris⁵⁹ of the split diffuse diffraction peaks observed in the system.^{32,60} Recently, one of us has generalized this explanation to all composition and temperatures using a one-dimensional Ising model in which repulsions at a distance $2a$ are essential.⁶¹

Moreover, experimental results for $x \sim 5/8$ (Refs. 32 and 29) suggest the structure of unit cell 1×8 shown in Fig. 2(a) of Ref. 1, which requires repulsions at a distance $7a$ to be stabilized. These longer-range repulsions modify drastically the transition temperatures.⁶²

An alternative starting point to the uncorrelated picture discussed in the previous paragraph is the purely ionic model for oxygen ordering.⁶³ As a consequence of the neglect of charge transfer, the ground state of this model for $x \sim 1/2$ contradicts experiment.^{29,33,47,50} This model was modified on the basis of electronic structure calculations in Ref. 1. In that work, a strong-coupling explanation of the hole count was given, all available diffraction patterns were explained, some of them were predicted,³² and thermodynamic properties were calculated. However, the analysis of each particular aspect was necessarily too brief and the recent neutron and x-ray experiments for $x \sim 3/8$ (Refs. 48, 49 and 51) render an estimation of the screening length λ necessary. For constant λ , the model of Ref. 1 predicts that the CS are present in the ground state symmetrically around $x \sim 1/2$, while the experimental data seems to favor HS for $x \sim 3/8$ (Refs. 29, 48, 49 and 51) and CS for $x \sim 5/8$.²⁹⁻³²

The objective of the present work is to show that, at least qualitatively for the moment, a harmonious strong-coupling explanation of the main peculiar electronic and structural properties of $\text{YBa}_2\text{Cu}_3\text{O}_{6+x}$ can be given, in which intra- and interatomic repulsions play a decisive role. Although our treatment is not fully self-consistent, the structural assumptions for the electronic model are consistent with both experiment and the results of the structural model, while the latter is proposed on the basis of the electronic structure calculations. In Sec. II we study the electronic structure of the CuO_x planes, including the apex O atoms, to obtain the distribution of holes and the energy gain ΔE which favors ordering in chains. In Sec. III, we calculate the screening length λ , using a one-band effective model for the CuO_2 planes and compare the energy of the CS and HS using a structural model which includes ΔE and λ . Section IV contains a comparison with experiment and discussion.

II. ELECTRONIC STRUCTURE OF THE CuO_{2+x} SUBSYSTEM

Before studying a more realistic model, we will discuss first the ionic limit [$t_{ij} = 0$ in Eq. (2)]. In this limit, the interplay between charge transfer and oxygen ordering and the decisive role of Cu intratomic (U_d) and Cu-O interatomic (U_{pd}) repulsions can be very easily understood. In Fig. 1, we show the structure (HS) which minimizes the total Coulomb repulsion energy under the assumption that all atoms related by symmetry operations in the tetragonal phase have the same charge^{63,41,42} for $x = 1/2$. We also show the structure composed of full and empty CuO chains (CS), which is actually the one experimentally observed for $x=1/2$.^{29,33,47,50,52} Let us assume that all O ions in the CuO_x planes and the apex O ions are present as O^{-2} . Let us also neglect for the moment the O-O repulsions. For CS there are two types of Cu

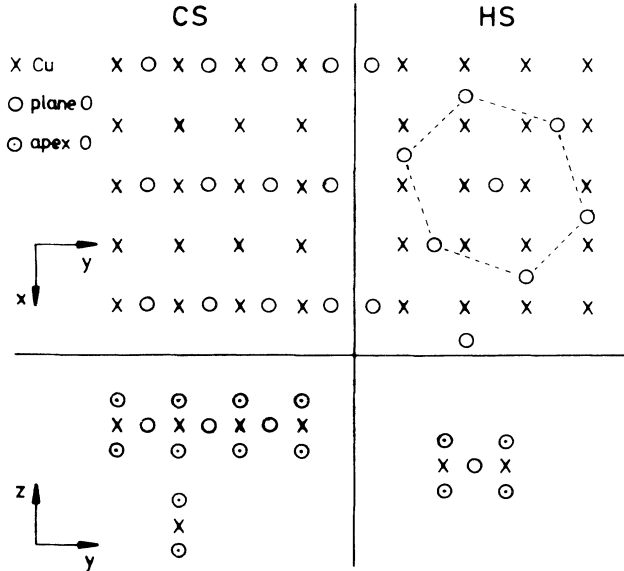


FIG. 1. Top: top view of the CuO_x planes for ordering in infinite CuO chains (left) and for the superstructure which minimizes the Coulomb repulsion energy between equally charged O atoms (right) for $x = 1/2$. Bottom: side view of the CuO_x planes showing the apex O atoms and the atomic structures which are electronically “disconnected” from the rest of the system.

atoms in the CuO_x planes: the fourfold coordinated and the twofold coordinated ones. To put the first hole in the former ones costs an energy $\epsilon_{\text{Cu}} - 8U_{pd}$, where the second term represents the attraction of the four nearest-neighbor O⁻² ions and ϵ_{Cu} , assumed site independent, contains all other interatomic interactions. Similarly for the twofold coordinated Cu ions, the energy necessary to convert them from Cu⁺ to Cu⁺² is $\epsilon_{\text{Cu}} - 4U_{pd}$. Due to the large intratomic repulsion U_d , the energy necessary to put the second hole on any Cu ion is very large and the Cu⁺³ configuration can be safely neglected in agreement with several studies.^{64,65} For HS, all Cu ions are threefold coordinated and the relevant energy levels lie at $\epsilon_{\text{Cu}} - 6U_{pd}$. The energy levels for both structures in the hole representation are shown in Fig. 2. When the superconducting CuO₂ planes are included, four different situations can occur depending on the value of the Fermi energy ϵ_F . If $\epsilon_F > \epsilon_{\text{Cu}} - 4U_{pd}$, all Cu ions are present as Cu⁺², no charge transfer to the planes takes place and the energy for CS and HS is the same. If however $\epsilon_{\text{Cu}} - 4U_{pd} > \epsilon_F > \epsilon_{\text{Cu}} - 6U_{pd}$, charge transfer takes place only for CS, the twofold coordinated Cu ions are Cu⁺, and the energy of CS is lower than that of HS by $\Delta E = \epsilon_{\text{Cu}} - 4U_{pd} - \epsilon_F$. In the other two situations $\epsilon_F < \epsilon_{\text{Cu}} - 6U_{pd}$ and for HS the charge in the superconducting planes per Cu is $2x$ and the amount of Cu⁺ is constant, contradicting several experimental evidence discussed later. For arbitrary concentrations, we define ΔE as the difference between the energy for HS and CS divided by the corresponding difference in four-fold coordinated Cu ions. ΔE can be interpreted as an energy

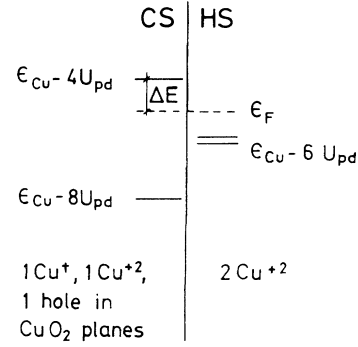


FIG. 2. Energy levels of the structures shown in Fig. 1 in the limit of vanishing hopping energy $t = 0$. The dashed line is a possible position of the Fermi level ϵ_f of the CuO₂ planes. At the bottom the corresponding charge distribution is indicated.

gain per pair of second-neighbor O atoms of the CuO_x planes with a Cu in between. We will use this interpretation in the next section.

The above simple picture with the Fermi level as in Fig. 2 provides a qualitative explanation of the doping effect of the ordering in chains,⁸⁻¹⁰ the effect of charge transfer in stabilizing the CS, and a $1-x$ ($1-2x$) dependence of the amount of Cu⁺ for CS (HS). However the position of the metal-insulator transition is not explained and the amount of charge in the superconducting CuO₂ planes is overestimated due to the neglect of covalency effects. To take these effects into account, we assume that the hopping between the apex O atoms and the atoms of the superconducting CuO₂ planes is weak enough to treat the CuO_x planes and the apex O atoms as an independent subsystem. This assumption is supported by band-structure calculations.³⁸⁻⁴⁰ One expects that this subsystem should be described in similar terms as the superconducting CuO₂ planes. There is a general consensus that the electronic structure of these planes is well described by the extended three-band Hubbard model⁶⁶⁻⁶⁸ (or effective models derived from it⁶⁹⁻⁷⁴). For the CuO_{2+x} subsystem with $x=1$, this model has the form

$$H = H_0 + H', \quad (1)$$

$$H_0(x=1) = \tilde{\epsilon}_d \sum_{i\sigma} d_{i\sigma}^\dagger d_{i\sigma} + \sum_{j\sigma} (\tilde{\epsilon}_d + \Delta_j) p_{j\sigma}^\dagger p_{j\sigma} + U_d \sum_i d_{i\uparrow}^\dagger d_{i\uparrow} d_{i\downarrow}^\dagger d_{i\downarrow} + U_p \sum_j p_{j\uparrow}^\dagger p_{j\uparrow} p_{j\downarrow}^\dagger p_{j\downarrow} + U_{pd} \sum_{i\delta\sigma\sigma'} d_{i\sigma}^\dagger d_{i\sigma} p_{i+\delta\sigma'}^\dagger p_{i+\delta\sigma'}, \quad (2)$$

$$H' = \sum_{i\delta\sigma} t_\delta (d_{i\sigma}^\dagger p_{i+\delta\sigma} + \text{H.c.}). \quad (3)$$

The sum over $i(j)$ extends over all Cu(O) atoms of the subsystem. Varying δ , $i + \delta$ labels the nearest-neighbor

(NN) chain or apex O atoms of the Cu atom located at site i . We assume that the relevant d and p orbitals are those pointing towards NN, as supported by ^{17}O NMR studies.⁷⁵ The phases of half of the d and p orbitals were changed so that all $t_\delta > 0$. We call $t_\delta = t$ for hopping in the CuO_x plane and take $t_\delta = t' = 1.28t$ for Cu-apex O hopping, using an $r^{-7/2}$ distance dependence.⁷⁶ Similarly we call $\Delta_j = \Delta$ if position j lies in the CuO_x plane and take $\Delta_j = \Delta + U_{pd}$ for apex O positions, so that if all Cu ions are Cu^{+2} , it takes the same energy to add a hole on a plane or on an apex O atom. This is suggested approximately by tight-binding fits to first-principles band-structure calculations.⁴⁰

The Hamiltonian given by Eqs. (1)–(3) is not appropriate for systems with $x \neq 1$ or another type of O ordering. On the one hand, if a Cu atom is a NN to two O atoms, which in turn are NN in the O plane sublattice, the assignment of the appropriate $3d$ e_g orbital on the basis of the NN configuration to the Cu atom is ambiguous. However, experimental⁷⁷ and theoretical^{1,78,62,79} evidence rule out the presence of NN O atoms in the CuO_x planes, even in the disordered tetragonal phase at moderate temperatures. On the other hand, if an O^{-2} ion of the CuO_x plane (i.e., without holes) is removed, it affects severely the energy necessary to add or remove holes in the neighborhood of the vacancy. This effect is not taken into account by the choice of vacuum reference state implicit in Eq. (2) and in alternative treatments of the problem.³⁵ Assuming that removal of *neutral* O atoms does not change the relevant energies, it is more convenient to express the interatomic repulsion in terms of the following Cu and O charge operators:

$$q_i = 1 + \sum_{\sigma} d_{i\sigma}^{\dagger} d_{i\sigma}, \quad q_j = -2 + \sum_{\sigma} p_{j\sigma}^{\dagger} p_{j\sigma}, \quad (4)$$

so that H_0 takes the form:

$$\begin{aligned} H_0 = & \epsilon_d \sum_{i\sigma} d_{i\sigma}^{\dagger} d_{i\sigma} + \epsilon_p \sum_{j1\sigma} p_{j1\sigma}^{\dagger} p_{j1\sigma} + \epsilon'_p \sum_{j2\sigma} p_{j2\sigma}^{\dagger} p_{j2\sigma} \\ & + U_d \sum_i d_{i\uparrow}^{\dagger} d_{i\uparrow} d_{i\downarrow}^{\dagger} d_{i\downarrow} + U_p \sum_j p_{j\uparrow}^{\dagger} p_{j\uparrow} p_{j\downarrow}^{\dagger} p_{j\downarrow} \\ & + U_{pd} \sum_{i\delta} q_i q_{i+\delta}, \end{aligned} \quad (5)$$

where the sum over $j1$ runs over all O atoms of the CuO_x

plane and that over $j2$ refers to apex O atoms. In order for Eq. (5) to coincide with Eq. (2) for $x=1$, the differences of on-site energies should be

$$\epsilon_p - \epsilon_d = \Delta - 10U_{pd}, \quad \epsilon'_p - \epsilon_p = 2U_{pd}. \quad (6)$$

In the rest of this section we compare the energy and the electronic properties of the model of Eqs. (1) and (3) to (6) for CS and HS as a function of oxygen composition x . What matters here about the structure is that, for CS, a fraction x of the Cu atoms lie in infinite CuO_3 chains, while the rest are contained in CuO_2 clusters (see Fig. 1). For HS and $x \leq 1/2$, $2x$ Cu atoms per original unit cell lie in Cu_2O_5 clusters, represented in the bottom of Fig. 1 at the right, while $1-2x$ Cu atoms lie in CuO_2 clusters. For $1/2 \leq x \leq 2/3$ (and for simplicity we extrapolate this behavior up to $x=1$), $2(1-x)$ Cu atoms of the HS lie in Cu_2O_5 clusters and $2x-1$ in infinite CuO_3 chains. Thus, the problem reduces to distribute the $2x$ holes brought by the O atoms among the superconducting CuO_2 planes and the available amount of CuO_2 clusters, Cu_2O_5 clusters, and infinite CuO_3 chains, minimizing the total energy. We further assume that for $x=0$, the CuO_2 planes have one hole per Cu atom, that to add further holes in these planes it is necessary to overcome a gap and that these holes have 80% O character and 20% Cu character.^{64,65} The energy necessary to add the first of these holes E_p is taken as a parameter, and a constant derivative of the energy with respect to the number of holes $\rho = \Delta/(4\pi t^2)$ is assumed for simplicity. The main results of this section are independent of this assumption. The finite clusters are calculated exactly. Infinite CuO_3 chains with one hole per Cu are simulated by a Cu_2O_6 cluster with periodic boundary conditions. However, this approximation is not good enough for higher doping levels and then we performed a canonical transformation eliminating H' (Refs. 72 and 73) to obtain an effective Hamiltonian H_{eff} for O holes and Cu spins (all Cu ions of the chain are Cu^{+2} and only virtual occupation of Cu^+ is allowed).

The detailed form of H_{eff} is practically the same as in Ref. 73 taking $U_d, U_p \rightarrow \infty$ as we assume. For a small number of added holes beyond one per Cu, H_{eff} can be written in the form (taking the origin of one-particle energies at $\tilde{\epsilon}_d=0$)

$$\begin{aligned} H_{\text{eff}} = & -N \sum_{\delta} t_{\delta}^2 / (\Delta + U_{pd}) + \sum_{j1\sigma} [\Delta + 2U_{pd} + 2t^2 / (\Delta + U_{pd})] p_{j1\sigma}^{\dagger} p_{j1\sigma} \\ & + \sum_{j2\sigma} [\Delta + 2U_{pd} + t'^2 / (\Delta + U_{pd})] p_{j2\sigma}^{\dagger} p_{j2\sigma} + \sum_{i\delta \neq \delta' \sigma'} (t_{\delta} t_{\delta'} / \Delta) d_{i\sigma}^{\dagger} d_{i\sigma'} p_{i+\delta, \sigma'}^{\dagger} p_{i+\delta, \sigma}. \end{aligned} \quad (7)$$

N is the number of Cu ions in the chain. The last term represents an effective hopping between two O atoms NN to a common Cu atom, accompanied by a Cu-O spin exchange. The magnitude of this hopping and the amount of Cu^+ is reduced significantly if corrections of higher

order in H' are included.⁷⁴ The construction of a more appropriate H_{eff} is in progress. Here we use the two approximations used in Ref. 34 and point out clearly which results depend on these approximations and in what way. The approximation 1 (2) for the dependence of the en-

ergy of the infinite chains with respect to the number of holes in them beyond one per Cu is a rigorous lower (upper) bound for the energy necessary to add the first of these holes. In approximation 1 we replace the last term of Eq. (7) by a hopping term without spin flip and *negative* sign. The idea is that a spin configuration would exist which for one added hole minimizes the energy taking *maximum* advantage of the effective hopping energy in the frustrated O sublattice. In approximation 2 all states with apex O occupation are neglected. Then, the sums over j_2 disappear and Eq. (7) reduces to the same Hamiltonian considered by Uimin *et al.*^{6,36} in the limit $U_d, U_p \rightarrow \infty$. In this limit the energy spectrum of the CuO chain (without apex O atoms) with open boundary conditions is independent of the spin configuration and can be obtained exactly.³⁴ Taking into account that the parameters of H_{eff} are overestimated,⁷⁴ approximation 2 is likely to be more realistic.

In Fig. 3 we show the hole distribution for reasonable parameter values. E_p was chosen so that for CS $n_H \sim 0.25$ in the plateau as experimentally observed.^{16,15} Similar curves can be obtained for other parameters choosing adequately E_p . If approximation 1 is used, lower values of t are necessary. For CS (HS) at the plateau, the Fermi energy is pinned at the energy necessary to add the second (third) hole to a CuO_2 (Cu_2O_5) cluster. As a consequence of the difference between these energies, the charge transfer to the planes is larger for CS. For both types of ordering, $n_H > 0$ for $x > 0.5$ and the semiconductor-superconductor transition takes place at $x=0.5$. The small structure at the left of the plateau in n_H for CS is due to a small occupancy of the "upper band" (beyond one hole per Cu) of the CuO_3 infinite chains. For CS and $x < 0.8$, the amount of Cu holes in the CuO_x planes ($n_{\text{Cu}} - 2$ in Fig. 3) varies as x . The deviation for $x > 0.8$ is due to delocalization of the Cu holes produced by the O occupation due to the large value of U_{pd} chosen. For lower values of U_{pd} and t , $n_{\text{Cu}} - 2$ approaches more the value x for CS. Instead, for HS, as it is clear at the limit $t=0$ explained at the beginning of this section, $n_{\text{Cu}} - 2$ approaches the behavior $2x$ for small x and lower values of t or larger values of Δ as those used in

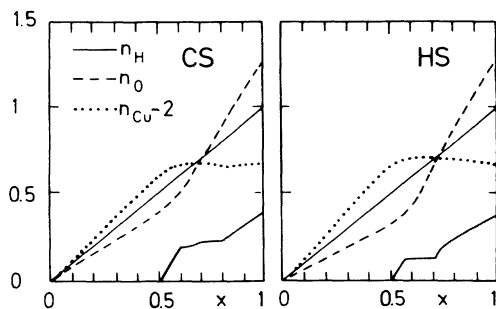


FIG. 3. Number of carriers in the planes n_H and total number of O (n_O) and Cu (n_{Cu}) holes per unit cell as a function of O content for ordering in chains (left) and for ordering with regularly spaced O atoms (right). Parameters are $t = 1$, $\Delta = 3$, $U_{pd} = 1.3$. Approximation 2 for doped CuO_3 chains was used. The thin line $n = x$ is a guide to the eye.

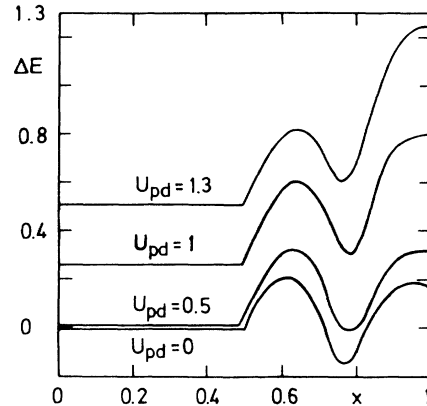


FIG. 4. Difference of energy between HS and CS divided by the difference in second-neighbor O atoms with a Cu in between, as a function of O content for several values of U_{pd} , $t = 1$, and $\Delta = 3$. Approximation 1 for doped CuO_3 chains was used, and the superconducting CuO_2 planes are assumed undoped for all x (see text).

Fig. 3. While n_H is the most interesting quantity for superconductivity, ΔE is one of the most relevant for the O ordering. Its dependence on x is illustrated in Fig. 4. For $x \leq 0.5$ the result depends only on the electronic structure of the CuO_2 and Cu_2O_5 clusters and the energy of the infinite CuO_3 chains for one hole per Cu. Thus, it is independent of the approximations used for the CuO_2 planes and doped chains. For $x > 0.5$, ΔE vs x increases (decreases) if approximation 1 (2) for doped chains is used and if the CuO_2 planes were undoped. Since, as shown before, the doping of the CuO_2 planes is larger for CS, this implies a larger decrease of the energy of CS and a tendency to increase ΔE as a consequence of doping, as in the example at the beginning of this section. Thus, we expect a slight increase of ΔE in the metallic phase, although a better treatment of doped chains is necessary to obtain quantitative results for $x > 0.5$. The dependence on U_{pd} is better illustrated in Fig. 5. In agreement

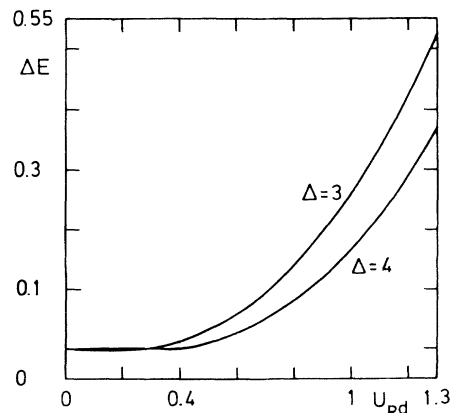


FIG. 5. Difference of energy between HS and CS divided by the difference in second-neighbor O atoms with a Cu in between, as a function of U_{pd} for $t = 1$, $x \leq 0.5$, and two values of Δ .

with the simple explanation in the limit $t=0$,⁴¹ $|\Delta E|$ is very small for $U_{pd} \rightarrow 0$ and decreases with increasing Δ . Assuming that the parameters t , U_{pd} , and Δ are similar to those obtained for La_2CuO_4 using constrained density functional calculations,^{69,80} the ratio U_{pd}/t lies between 0.37 and 1.3. Unfortunately because of this uncertainty, we can only say that $0 \lesssim \Delta E \lesssim 0.5$ in units of t .

III. ATOMIC STRUCTURE OF THE CuO_x PLANES

The structural model¹ assumes that any two i th NN O atoms of the planes (NN i) repel each other according to a screened Coulomb repulsion but the interaction between NN2 with a Cu atom in between $V_{2\text{Cu}}$ is reduced by ΔE calculated in the previous section, to take into account the effects of charge transfer. The model can be written as

$$H = \frac{1}{2} \sum_{ij} V_{i-j} n_i n_j, \quad (8)$$

n_i is the O occupation at site i ,

$$V_i = V \frac{\exp[-R_i/\lambda]}{R_i} \quad \text{but} \quad V_{2\text{Cu}} = V_2 - \Delta E, \quad (9)$$

$$V = \frac{q^2}{\epsilon a_0}, \quad (10)$$

R_i is the distance between NN i measured in units of the lattice parameter $a_0 = R_1 = a/\sqrt{2}$ of the sublattice of all possible O positions assumed square, λa_0 is the screening length, q is the O charge, and ϵ the dielectric constant in the semiconducting phase. We use $\epsilon = 14.7$ (Ref. 81) and $q = -1.7$.^{34,42} Using structural data³⁷ $a_0 = 2.76 \text{ \AA}$, then $V = 1.025 \text{ eV}$. The remaining parameter λ is calculated below. Since ΔE has its origin in the Cu-O NN repulsion U_{pd} , the model is based solely on Coulomb repulsions. It is justified in more detail in Refs. 41, 42 and 82. However, it is still oversimplified. It assumes that the effective interaction between the O atoms of the CuO_x planes and all other ions (except the NN Cu ones which are contained in ΔE) are independent of the O position. This is an approximation for the interactions within the CuO_{2+x} subsystem, since the charge of the Cu atoms of the CuO_x planes and its NN O apex ions depend on the coordination number of the Cu ions. Also, the assumed form of the dielectric and Thomas-Fermi screening is valid for large R_i , whereas at small distances different screening mechanisms (in addition to those taken into account in ΔE) take place.⁸³

The screening length can be estimated using Thomas-Fermi theory for an isotropic medium⁸⁴ which gives

$$\frac{1}{(\lambda a_0)^2} = 4\pi e^2 \frac{\partial \rho}{\partial \epsilon_F}, \quad (11)$$

where $\rho = n_H/(abc)$ is the number of carriers per unit volume. In terms of the number of holes per Cu ion of the superconducting CuO_2 planes we can write

$$\frac{\partial \rho}{\partial \epsilon_F} = \frac{2}{abc} \frac{dn}{d\epsilon_F} \quad (12)$$

and

$$\left(\frac{dn}{d\epsilon_F} \right)^{-1} = \frac{d\epsilon_F}{dn} = \frac{d^2 E}{dn^2}, \quad (13)$$

where E is the total energy per Cu ion of a CuO_2 plane. For a highly correlated system, E can be estimated using variational wave functions. We use the Gutzwiller approximation^{85,86} applied to an effective one-band model for CuO_2 planes.⁶⁹ Replacing for simplicity the unperturbed density of states by a rectangular band of the same width W , $E(n)$ is given by the minimum with respect to d of the function:

$$E(n, d) = -W(n/2 - d^2) [1 + 2d^2 - n + 2d(1 + d^2 - n)^{1/2}] + Ud^2, \quad (14)$$

where $W = 3.44 \text{ eV}$ and the effective Coulomb repulsion $U = 4.1 \text{ eV}$.⁶⁹ The last member of Eq. (14) is given by

$$\frac{d^2 E(n, d)}{dn^2} = \frac{\partial^2 E}{\partial n^2} - \left(\frac{\partial E}{\partial n \partial d} \right)^2 \left(\frac{\partial^2 E}{\partial d^2} \right)^{-1}. \quad (15)$$

Equations (11)–(13) and (15), and structural data³⁷ define λ for each value of $n_H = 2(n - 1)$. In the semiconducting phase one should have $\lambda = \infty$. For $0.5 \leq x \leq$

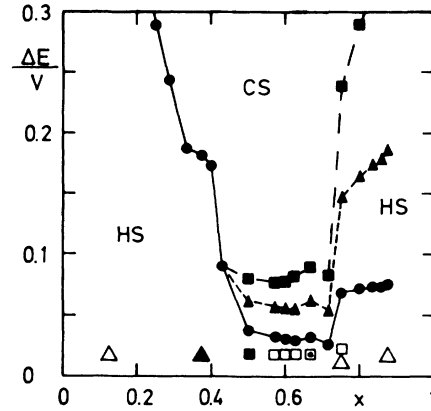


FIG. 6. Relative stability of superstructures (SS) composed of full and empty chains (CS) and those which minimize the Madelung free energy for uniformly charged ions (HS) in the $x, \Delta E$ plane. $\lambda = 10$ for $x \leq 3/7 = 0.43$ and for $x \geq 1/2$ $\lambda = 0.62$ (full line), $\lambda = 1$ (short-dashed line), and $\lambda = 2$ (long-dashed line) were chosen. Triangles at the bottom correspond to the ideal compositions for which electron-diffraction experiments which agree with HS were reported: $x = 1/8$ (Ref. 33), $3/8$ (Ref. 29), $3/4$ (Ref. 13), and $7/8$ (Ref. 33). The squares mean the same for CS: $x = 1/2$ (Refs. 29 and 33), $3/5$ (Refs. 30 and 32), $2/3$ (Refs. 31, 29, and 32), $4/7$, $5/8$ (Ref. 32) and $3/4$ (Refs. 29 and 32). Full symbols indicate that in addition x-ray experiments [$s = 3/8$ (Refs. 51 and 49), $x = 1/2$ (Ref. 50)] and neutron experiments [$x = 3/8$ (Refs. 48 and 49), $x = 1/2$ (Ref. 47)] confirming the character of the structure. For ideal composition $x = 2/3$, the SS has been confirmed by x-ray diffraction (Ref. 52). For $x = 3/8$, the SS are described in Fig. 7. For other compositions, the structures are represented in Refs. 41 and 42.

0.89, following Ref. 16 $n_H=0.24$. For this value of n_H we obtain $\lambda = 0.62$ ($\lambda a_0 = 1.68 \text{ \AA}$). This value is somewhat smaller than the one estimated in Ref. 87 and the value $\lambda \sim 1$ which leads to TG-OII transition temperature in reasonable agreement with experiment.⁶²

In Fig. 6 we represent the value of ΔE for which the energy of a CS is equal to the energy of the HS with the same composition. For the semiconducting phase we have taken $\lambda = 10$ [the results are practically insensitive to λ for $\lambda > 4$ (Ref. 42)], while in the metallic phase we have used the above-obtained value of λ and two other values. All possible CS with unit cell $1 \times n$ with $n \leq 8$ were considered.^{1,41,42} The HS are the ground state of the model of Eqs. (8) and (9) for $\Delta E = 0$.^{1,41,42} For some compositions, there are several different superstructures (SS), the energy which differs from the ground-state energy for $\Delta E = 0$ in less than $V/100$.^{41,42,46} Here we extend the term HS to all these quasidegenerate SS. Examples are the SS shown in Figs. 7(c)-7(f).⁴⁶ In a small interval of ΔE , SS which consist of short

O-Cu-O segments [such as the SS shown in Fig. 7(b)] are the ground state.^{1,41,42} We call them PS. Neglecting these PS, Fig. 6 is practically a ground-state phase diagram. Actually, the PS of Fig. 7(b) is the ground state for $0.12 < \Delta E/V < 0.31$,⁴² and will be taken into account in the discussion of the next section. The abrupt decrease for $x \sim 0.45$ in the critical value of ΔE (ΔE_c) necessary to stabilize the CS is due to the decrease of λ (metal-insulator transition), while the increase of ΔE_c for $x \sim 0.74$ is due to the change in the form of the HS: for $x \leq 2/3$ they consist of regularly spaced O atoms (such as Fig. 1 right), while for $x \geq 3/4$, they can be thought as a (nearly hexagonal) pattern of additional O vacancies added to the CS with $x=1$.^{1,41}

IV. COMPARISON WITH EXPERIMENTS

Concerning structural information, all diffraction patterns so far reported are compatible with either HS or CS. The character of the observed SS for each composition is indicated in Fig. 6. The electron-diffraction results except those for $x=1/2$ have been objected: For $x > 0.5$ it has been suggested that the observed SS are produced by the electron-beam heating,²⁹ while for O lean samples, physical phenomena different from O ordering were used to explain the data.^{88,89} However, the neutron-diffraction SS peaks measured for $x \sim 3/8$ are clearly due to O ordering.⁴⁸ The observed intensities are proportional to the square of the O form factor. They are reproduced in Table I together with the corresponding theoretical results for the three SS represented in Fig. 1, which are able to reproduce the two most intense peaks [for two-dimensional wave vectors $(1/2, 1/2)$ and $(3/2, 3/2)$]. Note that NN2 interfere destructively for these reflections and then SS containing O-Cu-O segments such as those represented in Fig. 7(a) or 7(b) cannot explain the data. The same conclusion is reached from the x-ray experiments,^{51,49} although they require one to take into account Cu displacements for their interpretation. While the x-ray experiments are fully compatible with the SS of Fig. 7(e),⁴⁹ the neutron experiments favor the SS of Fig. 7(f) (see Table I). The model of Ref. 1 also favors it,⁴⁶ but on an energy scale less than $V/100$, other interactions, such as elastic energies^{90,82} become important and might determine the SS of less free energy. In fact, although the samples used in the neutron and x-ray experiments were taken from the same crystal, the measured lattice parameters are slightly different,^{48,51} suggesting that the observed SS might be different microstructures, one of them slightly excited with respect to the other. Note that if the interaction between NN2 were attractive ($V_{2Cu} < 0$), both SS would be *unstable* against NN O displacements. Monte Carlo calculations confirm that metastable SS obtained assuming $V_{2Cu} < 0$ always have short O-Cu-O segments and are thus incompatible with the neutron and x-ray experiments for $x \sim 3/8$.^{87,91} Moreover V_{2Cu} should be positive and large enough to avoid that the SS of Fig. 7(b) be the ground state.^{41,42} Note that it is the ground state for the parameters chosen in a recent calculation of the structure transformation kinetics.⁸²

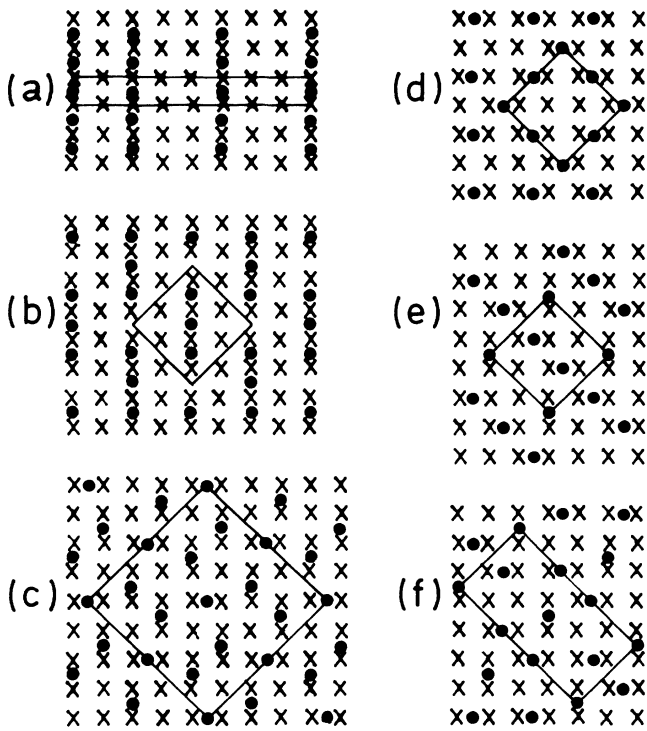


FIG. 7. Several superstructures for $x = 3/8$. (a) CS which is the ground state of the model of Ref. 1 for large ΔE , (b) ground state of the model for intermediate values of ΔE , called PS (Refs. 41, 42, and 82), (c)-(g) structures with nearly the ground-state energy for $\Delta E = 0$, (c) is the one of minimum energy (Ref. 46). (d) was proposed on the basis of electron-diffraction (Ref. 29) and neutron-diffraction (Ref. 48) experiments. (e) is the one of minimum energy among all those $2\sqrt{2} \times 2\sqrt{2}$ superstructures (Refs. 41, 42, and 46) and the one which best explains the x-ray experiments (Ref. 49). (f) is the one of less free energy near room temperatures and the one which best explains the neutron experiments (Ref. 46). Thin full lines delimit unit cells.

TABLE I. Observed neutron-diffraction intensities in counts for $x \sim 3/8$ and wave vectors $(2\pi/a)(h, k, 0)$ with $0 \leq k \leq h \leq 7/4$ and $4h, 4k$ integers (Ref. 48), in comparison with the corresponding intensities for the SS shown in Figs. 7(d)–(f). The temperature factor was chosen to fit the two most intensely observed peaks. The results are the same if h and k are interchanged. 2θ is the scattering angle, $\sigma = 10$ the reported statistical error, and msd the mean square deviation between observed and calculated intensities. The intensities for which all reflections in the different atoms of the SS interfere constructively are underlined.

h	k	2θ	I_{obs}	I_d	I_e	I_f
1/4	1/4	12		93	93	0
1/2	0	18	40	65	65	0
1/2	1/2	25	420	<u>420</u>	<u>420</u>	<u>420</u>
3/4	1/4	28	50	41	41	41
3/4	3/4	38	$< \sigma$	31	31	0
1	1/2	40	$< \sigma$	29	29	0
5/4	1/4	46	$< \sigma$	26	<u>235</u>	0
5/4	3/4	53	$< \sigma$	22	22	22
3/2	0	55	$< \sigma$	22	22	0
3/2	1/2	58	30	<u>191</u>	21	21
5/4	5/4	66	$< \sigma$	19	19	0
7/4	1/4	66	$< \sigma$	19	19	19
3/2	1	67	$< \sigma$	18	18	0
7/4	3/4	72	$< \sigma$	18	<u>163</u>	0
3/2	3/2	81	150	<u>150</u>	<u>150</u>	<u>150</u>
7/4	5/4	83	$< \sigma$	16	16	16
7/4	7/4	99		15	15	0
msd				43	71	12

In spite of the controversy on the electron-diffraction results, it is encouraging to find that there is a range of ΔE for which all the structural data, except one of the conflicting results for $x = 3/4$, can be explained. As seen in Fig. 6, for $\lambda = 0.62$ estimated in the previous section, the above-mentioned range is $0.038 < \Delta E/V < 0.069$. If $\lambda = 1$ this range increases to $0.062 < \Delta E/V < 0.147$ [however for $\Delta E/V > 0.12$, the structural model predicts the SS of Fig. 7(b) as the ground state for $x = 3/8$ contrary to experiment]. This range of values is in agreement with recent results in which the composition dependence of the superconducting critical temperature T_c can be explained using an empirical relationship between T_c and Madelung potentials if and only if HS for $x \leq 2/5$ and $x \geq 3/4$ are assumed.⁴ The results of Sec. II, as well as other studies^{5,6,8–10} suggest that CS ordering favors charge transfer and the metallization of the system. In turn, results of the last section and the above analysis suggest that as x increases, a transition from HS to CS takes place, together with the insulator-metal transition. This coincidence is suggested by combined measurements of lattice parameters and transport properties,^{15,14,92} although they cannot distinguish between an HS or a disordered TG phase.

In contrast to the TG-OII transition, the HS-OII transition should be discontinuous. Evidence for a first-order transition around $x \sim 0.35$ in $\text{ErBa}_2\text{Cu}_3\text{O}_{6+x}$ has been found recently.⁹³ Also, between 0.2 and 0.4, the amount of Cu^+ in $\text{YBa}_2\text{Cu}_3\text{O}_{6+x}$ changes from a $1-2x$ dependence to a $1-x$ dependence.^{20,21} As shown in Sec. II, this is consistent with a transition between HS to CS with increasing x . Further evidence of this transition is provided by Raman spectra measurements:⁹⁴ a mode re-

lated to apex O vibrations NN to fourfold coordinated Cu ions, observed for $x \gtrsim 0.5$ around 500 cm^{-1} , is seen to rapidly decrease in intensity and disappear with decreasing x near the metal-insulator transition. The absence of fourfold coordinated Cu ions in the semiconducting phase is only possible for ordering in HS. A disordered TG phase for x such that the ground state is a CS has a large amount of fourfold coordinated Cu ions due to short-range correlations.^{1,78,62} Nuclear quadrupole resonance experiments of Cu and their interpretation⁹⁵ also support the presence of predominantly threefold coordinated Cu ions in the semiconducting phase.

Other interesting experiments which show the relationship between the atomic and the electronic structure of $\text{YBa}_2\text{Cu}_3\text{O}_{6+x}$ are the observation of photoinduced changes in the transport properties of thin films.^{96–98} The resistivity of thin films of $\text{YBa}_2\text{Cu}_3\text{O}_{6+x}$ with $x \sim 0.4$ decreases and T_c increases as a consequence of illumination. When illumination ceases at room temperature, the transport properties return to their original values before illumination with times characteristic of O diffusion. We propose the following explanation: the ground state for the experimental composition is an ordered HS [or PS like Fig. 7(b)]. Illumination promotes carriers to the superconducting CuO_2 planes, producing the observed changes in the transport properties and lowering the screening length. As a consequence of this, the SS becomes unstable and simultaneously with the illumination, ordering in CS takes place. When illumination ceases the opposite processes occur. An alternative explanation, based on photoassisted O ordering assumes that the ground state is a CS, and that the original state is a disordered metastable one.^{98,99} This explanation re-

quires a phase transition to the disordered phase in the relaxation process after ceasing the illumination and, as pointed out in Ref. 97 it is not clear why the final state is so different from the disordered one produced by quenching according to the transport properties.

In addition to its relevance for a qualitative understanding of the O ordering in $\text{YBa}_2\text{Cu}_3\text{O}_{6+x}$, the structural model¹ [Eqs. (8) and (9)] is of interest by itself. For large values of λ , one expects that the temperature (T) composition (x) phase diagram at low T is characterized by a dense sequence of first-order transitions with two-phase fields of vanishing width in composition.^{41,82} In other words, we expect that the ground state for any rational value of x is not a mixture of two phases, but a well-defined characteristic superstructure. This is suggested by the results of Ref. 41 and the exact solution of the ground state of the one-dimensional (1D) Ising model with interactions satisfying $2V_n < V_{n-1} + V_{n+1}$.^{100,101} At low enough T , and for compositions for which the ground state of the model of Ref. 1 is a CS, the model can be mapped into the above-described 1D Ising model.¹⁰² Considering in this model only V_1 and V_2 , the resulting diffraction spectra explain very well the diffuse peaks observed in $\text{YBa}_2\text{Cu}_3\text{O}_{6+x}$ for all x and T .⁶¹ Also, the principal modulation vector estimated from two-dimensional Monte Carlo simulations shows a dependence on the O chemical potential which strongly suggests the presence of a complete devil's staircase.¹⁰³

According to our results in Sec. II, the plateau in n_H vs x and the 60 K plateau of T_c vs x are due to the fact that the Fermi level is pinned at values determined by many-body levels of CuO_2 clusters for CS and

Cu_2O_5 clusters for HS. This explanation seems consistent with the description of T_c for intermediate values of x when Y is replaced by larger ions.^{92,104-106} This substitution enlarges the Cu-O distances in the superconducting CuO_2 planes, but does not modify substantially the distance between Cu atoms of the CuO_x planes and apex O atoms.³⁷ Thus, one expects a narrower band for the CuO_2 planes due to the distance dependence of the hopping⁷⁶ and a smaller amount of charge transfer to them. Similarly for CS ordering one expects that uniaxial pressure in the a direction broadens the superconducting band without affecting the chains, increasing the charge transfer to it and decreasing T_c at compositions $x \gtrsim 0.9$ for which the system is overdoped. This is in qualitative agreement with experiment.^{27,107-110} The effect of partial isomorphous substitutions can be understood in similar terms.¹¹¹ However, the composition dependence of the strain derivatives of T_c (Ref. 110) are difficult to explain and it might be necessary to take into account the stress dependence of other parameters.

A more quantitative study of the electronic properties in the metallic region requires a better description of the doped infinite CuO_3 chains. On a qualitative level our results agree with the most peculiar experimental observations in $\text{YBa}_2\text{Cu}_3\text{O}_{6+x}$. These electronic calculations allow an estimate of the parameters of the structural model of Ref. 1. Within the range of uncertainty of these parameters, one can find reasonable sets of values for which the structural model explains most of the reported diffraction data (in particular for $x \sim 3/8$ and $x \sim 1/2$) and thermodynamics.⁶²

¹A.A. Aligia, J. Garcés, and H. Bonadeo, Phys. Rev. B **42**, 10 226 (1990).

²L.F. Feiner and D.M. de Leeuw, Solid State Commun. **70**, 1165 (1989).

³J. Kondo, J. Phys. Soc. Jpn. **59**, 819 (1990).

⁴Qiang Wang, Han Rushan, D.L. Yin, and Z.Z. Gan, Phys. Rev. B **45**, 10 834 (1992).

⁵R.P. Gupta and M. Gupta, Phys. Rev. B **44**, 2739 (1991).

⁶G.V. Uimin, V.F. Gantmakher, A.M. Neminsky, L.A. Novomlinsky, D.V. Shovkun, and P. Brüll, Physica C **192**, 481 (1992).

⁷V.E. Zubkus, G.M. Vujičić, P.J. Kundrotas, and V.V. Tatarskij, Phys. Rev. B **45**, 10 728 (1992).

⁸B.W. Veal, A.P. Paulikas, Hoydoo You, Hao Shi, Y. Fang, and J.W. Downey, Phys. Rev. B **42**, 6305 (1990).

⁹H. Claus, S. Yang, A.P. Paulikas, J.W. Downey, and B.W. Veal, Physica C **171**, 205 (1990).

¹⁰S. Libbrecht, E. Osquiguil, B. Wuyts, M. Maenhoudt, Z.X. Gao, and Y. Bruynseraede, Physica C **206**, 51 (1993).

¹¹J. Kircher, E. Brücher, E. Schönherr, R.K. Kremer, and M. Cardona, Phys. Rev. B **46**, 588 (1992).

¹²R.J. Cava, B. Batlogg, C.H. Chen, E.A. Rietman, S.M. Zahurak, and D. Werder, Phys. Rev. B **36**, 5719 (1987).

¹³C.N.R. Rao, R. Nagarajan, A.K. Ganguli, G.N. Subbana, and S.V. Bhat, Phys. Rev. B **42**, 6765 (1990).

¹⁴V.E. Zubkus, O.E. Parfionov, E.E. Tornau, and P.J. Kun-

drotas, Physica C **198**, 141 (1992).

¹⁵O.E. Parfionov and A.A. Konovalov, Physica C **202**, 385 (1992), and references therein.

¹⁶Z.Z. Wang, J. Clayhold, N.P. Ong, J.M. Tarascon, L.H. Greene, W.R. McKinnon, and G.W. Hull, Phys. Rev. B **36**, 7222 (1987).

¹⁷Y. Tokura, J.B. Torrance, T.C. Huang, and A.I. Nazzari, Phys. Rev. B **38**, 7156 (1988).

¹⁸J. Rossat-Mignod, L.P. Regnault, M.J. Jurgens, C. Vettier, P. Burlet, J.Y. Henry, and G. Lapertot, Physica B **163**, 4 (1990).

¹⁹G. Cannelli, M. Canali, R. Cantelli, F. Cordero, S. Ferraro, M. Ferretti, and F. Trequattrini, Phys. Rev. B **45**, 931 (1992).

²⁰J.M. Tranquada, S.M. Heald, A.R. Moodenbaugh, and Y. Xu, Phys. Rev. B **38**, 8893 (1988).

²¹H. Tolentino, A. Fontaine, F. Baudalet, T. Gourieux, G. Krill, J.Y. Henry, and J. Rossat-Mignod, Physica C **192**, 115 (1992).

²²W.W. Warren, Jr., R.E. Walstedt, G.F. Brennert, R.J. Cava, B. Batlogg, and L.W. Rupp, Phys. Rev. B **39**, 831 (1989).

²³J.J. Neumeier, T. Bjorholm, M.B. Maple, and I.K. Schuller, Phys. Rev. Lett. **63**, 371 (1989).

²⁴J.L. Tallon and G.M. Williams, J. Less-Common Met. **164-165**, 70 (1990).

- ²⁵J.L. Tallon and N.E. Flower, *Physica C* **204**, 237 (1993).
- ²⁶C.C. Almasan, S.H. Han, B.W. Lee, L.M. Paulius, M.B. Maple, B.W. Veal, J.W. Downey, A.P. Paulikas, Z. Fisk, and J.E. Schirber, *Phys. Rev. Lett.* **69**, 680 (1992).
- ²⁷J.J. Neumeier and H.A. Zimmermann, *Phys. Rev. B* **47**, 8385 (1993).
- ²⁸J. Zaanen, A.T. Paxton, O. Jepsen, and O.K. Andersen, *Phys. Rev. Lett.* **60**, 2685 (1988).
- ²⁹J. Reyes-Gasga, T. Krekels, G. Van Tendeloo, J. Van Landuyt, S. Amelinckx, W. H.M. Bruggink, and H. Verweij, *Physica C* **159**, 831 (1989), and references therein.
- ³⁰D.J. Werder, C.H. Chen, R.J. Cava, and B. Batlogg, *Phys. Rev. B* **37**, 2317 (1988).
- ³¹D.J. Werder, C.H. Chen, R.J. Cava, and B. Batlogg, *Phys. Rev. B* **38**, 5130 (1988).
- ³²R. Beyers, B.T. Ahn, G. Gorman, V.Y. Lee, S.S.P. Parkin, M.L. Ramirez, K.P. Roche, J.E. Vazquez, T.M. Gür, and R.A. Huggins, *Nature* **340**, 619 (1989).
- ³³M.A. Alario-Franco, C. Chaillout, J.J. Capponi, J. Chenavas, and M. Marezio, *Physica C* **156**, 455 (1988), and references therein.
- ³⁴A.A. Aligia, *Solid State Commun.* **78**, 739 (1991).
- ³⁵A. Latgé, E.V. Anda, and J.L. Morán-López, *Phys. Rev. B* **42**, 4288 (1990).
- ³⁶G. Uimin and J. Rossat-Mignod, *Physica C* **199**, 251 (1992).
- ³⁷M. Guillaume, P. Allenspach, J. Mesot, B. Roessli, U. Staub, P. Fischer, and A. Furrer, *Z. Phys. B* **90**, 13 (1993).
- ³⁸L.F. Mattheis and D.R. Hamann, *Solid State Commun.* **63**, 395 (1987).
- ³⁹V.I. Anisimov and M.A. Korotin, *Problems of High-Temperature Superconductivity* (USSR Acad. Sci., Sverdlovsk, 1988), Issue 7.
- ⁴⁰M.J. De Weert, D.A. Papaconstantopoulos, and W.E. Pickett, *Phys. Rev. B* **39**, 4235 (1989).
- ⁴¹A.A. Aligia, H. Bonadeo, and J. Garcés, *Phys. Rev. B* **43**, 542 (1991).
- ⁴²A.A. Aligia, J. Garcés, and H. Bonadeo, *Physica C* **190**, 234 (1992).
- ⁴³P. Schleger, W.N. Hardy, and B.X. Yang, *Physica C* **176**, 261 (1991).
- ⁴⁴H.F. Poulsen, N.H. Andersen, and B. Lebech, *Physica C* **173**, 387 (1991).
- ⁴⁵D.K. Hilton, B.M. Gorman, P.A. Rikvold, and M.A. Novotny, *Phys. Rev. B* **46**, 381 (1992), and references therein.
- ⁴⁶A.A. Aligia, *Europhys. Lett.* **18**, 181 (1992).
- ⁴⁷Y.P. Lin, J.E. Greedan, A.H. O'Reilly, J.N. Reimers, and C.V. Stager, *J. Solid State Chem.* **84**, 226 (1990).
- ⁴⁸R. Sonntag, D. Hohlwein, T. Brückel, and G. Collin, *Phys. Rev. Lett.* **66**, 1497 (1991).
- ⁴⁹R. Sonntag, Th. Zeiske, and D. Hohlwein, *Physica B* **180-181**, 374 (1992).
- ⁵⁰R.M. Fleming, L.F. Schneemeyer, P.K. Gallagher, B. Batlogg, L.W. Rupp, and J.V. Waszczak, *Phys. Rev. B* **37**, 7920 (1988).
- ⁵¹Th. Zeiske, D. Hohlwein, R. Sonntag, F. Kubanek, and G. Collin, *Z. Phys. B* **86** 11 (1992).
- ⁵²V. Plakhty, A. Stratilatov, Yu. Chernikov, V. Federov, S.K. Sinha, C.K. Loong, B. Gaulin, M. Vlasov, and S. Moshkin, *Solid State Commun.* **84**, 639 (1992).
- ⁵³See, for example, J.M. Sanchez, J.P. Sark, and V.L. Moruzzi, *Phys. Rev. B* **44**, 5411 (1991); C. Sigli, M. Kosugi, and J.M. Sanchez, *Phys. Rev. Lett.* **57**, 253 (1986), and references therein.
- ⁵⁴A. Fernández Guillermet, J. Häglund, and G. Grimvall, *Phys. Rev. B* **45**, 11 557 (1992).
- ⁵⁵V.I. Anisimov, M.A. Korotin, J. Zaanen, and O.K. Andersen, *Phys. Rev. Lett.* **68**, 345 (1992).
- ⁵⁶P.A. Sterne and L.T. Wille, *Physica C* **162-164**, 223 (1989).
- ⁵⁷E. Pörschke, P. Meuffels, and H. Wenzl, *J. Phys. Chem. Solids* **53**, 73 (1992).
- ⁵⁸A.A. Aligia, *Phys. Rev. Lett.* **65**, 2475 (1990).
- ⁵⁹A.G. Khachaturyan and J.W. Morris, Jr., *Phys. Rev. Lett.* **64**, 77 (1990).
- ⁶⁰L.E. Levine and M. Däumling, *Phys. Rev. B* **45**, 8146 (1992).
- ⁶¹A.A. Aligia, *Phys. Rev. B* **47**, 15 308 (1993).
- ⁶²A.A. Aligia and J. Garcés, *Physica C* **194**, 223 (1992). If λ depends on x , the phase diagram is modified in a similar way as in Ref. 14.
- ⁶³A.A. Aligia, A.G. Rojo, and B. Alascio, *Phys. Rev. B* **38**, 6604 (1988).
- ⁶⁴J.C. Fuggle, J. Fink, and N. Nücker, *Int. J. Mod. Phys. B* **2**, 1185 (1988).
- ⁶⁵G. Bubeck, A.M. Olés, and M.C. Böhm, *Z. Phys. B* **76**, 143 (1989).
- ⁶⁶V.J. Emery, *Phys. Rev. Lett.* **58**, 2794 (1987).
- ⁶⁷P.B. Littlewood, C.M. Varma, and E. Abrahams, *Phys. Rev. Lett.* **63**, 2602 (1989), and references therein.
- ⁶⁸G. Dopf, J. Wagner, P. Dieterich, A. Muramatsu, and W. Hanke, *Phys. Rev. Lett.* **68**, 2082 (1992), and references therein.
- ⁶⁹M.S. Hybertsen, E.B. Stechel, W.M.C. Foulkes, and M. Schlüter, *Phys. Rev. B* **45**, 10 032 (1992).
- ⁷⁰H.B. Schüttler and A.J. Fedro, *Phys. Rev. B* **45**, 7588 (1992).
- ⁷¹M.E. Simón, M. Balina, and A.A. Aligia, *Physica C* **206**, 297 (1993).
- ⁷²V.J. Emery and G. Reiter, *Phys. Rev. B* **38**, 11 938 (1988).
- ⁷³C.D. Batista and A.A. Aligia, *Solid State Commun.* **83**, 11 938 (1992).
- ⁷⁴C.D. Batista and A.A. Aligia, *Phys. Rev. B* **47**, 8929 (1993).
- ⁷⁵M. Takigawa, P.C. Hammel, R.H. Heffner, Z. Fisk, K.C. Ott, and J.D. Thompson, *Phys. Rev. Lett.* **63**, 1865 (1989).
- ⁷⁶W.A. Harrison and S. Froyen, *Phys. Rev. B* **21**, 3214 (1980).
- ⁷⁷W.R. McKinnon, M.L. Post, L.S. Selwyn, G. Pleizier, J.M. Tarascon, P. Barboux, L.H. Greene, and G.W. Hull, *Phys. Rev. B* **38**, 6543 (1988).
- ⁷⁸A.A. Aligia and J. Garcés, *Phys. Rev. B* **44**, 7102 (1991).
- ⁷⁹V.E. Zubkus, E.E. Tornau, S. Lapinskas, and P.J. Kundrotas, *Phys. Rev. B* **43**, 13 112 (1991).
- ⁸⁰J.F. Annett, R.M. Martin, A.K. McMahan, and S. Satpathy, *Phys. Rev. B* **40**, 2620 (1989), and references therein.
- ⁸¹G.A. Samara, W.F. Hammetter, and E.L. Venturini, *Phys. Rev. B* **41**, 8974 (1990).
- ⁸²S. Semenovskaya and A.G. Khachaturyan, *Phys. Rev. B* **46**, 6511 (1992).
- ⁸³J. Oliva, *Phys. Rev. B* **35**, 3431 (1987).
- ⁸⁴N.W. Ashcroft and N.D. Mermin, *Solid State Physics* (Holt, Rinehart, and Winston, New York, 1976).
- ⁸⁵M.C. Gutzwiller, *Phys. Rev.* **137**, A1726 (1965).
- ⁸⁶D. Vollhardt, *Rev. Mod. Phys.* **56**, 99 (1984).
- ⁸⁷Zhi-Xiong Cai and S.D. Mahanti, *Phys. Rev. B* **40**, 6558 (1989).

- ⁸⁸T. Krekels, T.S. Shi, J. Reyes-Gasga, G. Van Tendeloo, J. Van Landuyt, and S. Amelinckx, *Physica C* **167**, 677 (1990).
- ⁸⁹D.J. Werder, C.H. Chen, and G.P. Espinosa, *Physica C* **173**, 285 (1991).
- ⁹⁰S. Semenovskaya and A.G. Khachatryan, *Phys. Rev. Lett.* **67**, 2223 (1991).
- ⁹¹C.P. Burmester and L.T. Wille, *Phys. Rev. B* **40**, 8795 (1989).
- ⁹²H. Shaked, B.W. Veal, J. Faber, Jr., R.L. Hitterman, V. Balachandran, G. Tomlins, H. Shi, L. Morss, and A.P. Paulikas, *Phys. Rev. B* **41**, 4173 (1990).
- ⁹³P.G. Radaelli, C.U. Segre, D.G. Hinks, and J.D. Jorgensen, *Phys. Rev. B* **45**, 4923 (1992).
- ⁹⁴G. Burns, F.H. Dacol, C. Field, and F. Holtzberg, *Solid State Commun.* **77**, 367 (1991).
- ⁹⁵V.S. Kasperovich and E.V. Charnaya, *Fiz. Tverd. Tela* **34**, 2040 (1992) [*Sov. Phys. Solid State* **34**, 1089 (1992)].
- ⁹⁶V.I. Kudinov, I.L. Chaplygin, A.I. Kirilyuk, N.M. Kreines, R. Laiho, and E. Lähderanta, *Phys. Lett. A* **157**, 290 (1991).
- ⁹⁷G. Nieva, E. Osquiguil, J. Guimpel, M. Maenhoudt, B. Wuyts, Y. Bruynseraede, M.B. Maple, and I.K. Schuller, *Phys. Rev. B* **46**, 14 249 (1992).
- ⁹⁸K. Kawamoto, H. Masuda, K. Natsume, N. Honma, I. Hirabayashi, T. Morishita, and S. Tanaka, in *Advances in Superconductivity IV*, edited by H. Hayakawa and N. Koshizuka (Springer-Verlag, Tokyo, 1992), p. 143.
- ⁹⁹E. Osquiguil (private communication).
- ¹⁰⁰V.L. Pokrovsky and G.V. Uimin, *J. Phys. C* **11**, 3535 (1978).
- ¹⁰¹J. Hubbard, *Phys. Rev. B* **17**, 494 (1978).
- ¹⁰²A.A. Aligia, J. Garcés, and J.P. Abriata (unpublished).
- ¹⁰³D. Adelman, C.P. Burmester, L.T. Wille, P.A. Sterne, and R. Gronsky, *J. Phys.* **4**, L585 (1992).
- ¹⁰⁴M. Buchgeister, W. Hiller, S.M. Hosseini, K. Kopitzki, and D. Wagener, in *Progress in High Temperature Physics*, edited by R. Nicolisky (World Scientific, Singapore, 1990), Vol. 25, p. 511.
- ¹⁰⁵M. Kogachi, S. Nakanishi, K. Nakahigashi, H. Susakura, S. Minamigawa, N. Fukuoka, and A. Yanese, *Jpn. J. Appl. Phys.* **28**, L609 (1989).
- ¹⁰⁶B.W. Veal, A.P. Paulikas, J.W. Downey, H. Claus, K. Vanderwort, G. Tomlins, H. Shi, M. Jensen, and L. Morss, *Physica C* **162-164**, 97 (1989).
- ¹⁰⁷S.L. Bud'ko, J. Guimpel, O. Nakamura, M.B. Maple, and I.K. Schuller, *Phys. Rev. B* **46**, 1257 (1992).
- ¹⁰⁸U. Welp, M. Grimsditch, S. Fleshler, W. Nessler, J. Downey, G.W. Crabtree, and J. Guimpel, *Phys. Rev. Lett.* **69**, 2130 (1992).
- ¹⁰⁹M. Kund and K. Andres, *Physica C* **205**, 32 (1993).
- ¹¹⁰O. Kraut, C. Meingast, G. Bräuchle, H. Claus, A. Erb, G. Müller-Vogt, and H. Wühl, *Physica C* **205**, 139 (1993).
- ¹¹¹M. Kakihana, S.G. Erikson, L. Börjesson, L.G. Johansson, C. Ström, and M. Käll, *Phys. Rev. B* **47**, 5359 (1993).